

First-principle studies of the electronic band structure and the phonon dispersion properties of wurtzite BN

X. Lei, X. X. Liang, G. J. Zhao, and T. L. Song

Department of Physics, School of Physical Science and Technology, Inner Mongolia University, Hohhot, 010021, P. R. China

E-mail: xxliang@imu.edu.cn

Abstract. The electronic band structure and phonon dispersion of wurtzite BN are studied by the first principle calculations. The local density approximation (LDA) and the generalized gradient approximation (GGA) exchange-correlation potentials are applied in the calculations and compared. The computational results for the band structure and density of states with indirect band gaps as well as the phonon dispersive curves and density of states are obtained. The corresponding dielectric and thermodynamic properties are discussed. The conclusions are consistent with other theoretical results and experimental data.

1. Introduction

In recent years Group-III nitride compound semiconductors have been widely studied due to their important device applications [1-3]. Boron nitride (BN), as a kind of III-N semiconductors, has attracted experimental and theoretical interests. The basic crystallographic structures of BN are hexagonal wurtzite (WZ) and cubic zincblende (ZB) structures [4-6] and the former usually more stable. The electronic band structure of wurtzite BN have been studied by first-principle calculations. The calculated results for the band gap are generally slightly smaller than experimental results of around 5.0 eV. Attention has also been paid to the lattice vibrations (phonons), which related closely to their electric, optical as well as thermal properties. Some authors have calculated the phonon dispersions of hexagonal BN by the first-principles with the tight-binding method [7,8]. Second-order Raman scattering has been used to probe phonon dispersions away from the Γ point [9].

In present work a first-principle calculation has been employed to obtain the band structure, state densities of electrons as well as the phonon dispersion curves of the WZ-BN. The corresponding dielectric and thermodynamic properties are discussed in brief.

2. Calculation method

The Plane Wave Self Consistent Field (PWscf) method of Quantum-Espresso [10] is used, by employing the plane wave basis set and the pseudo potential different from previous calculations. Computations are performed by means of the density functional theory (DFT) in conjunction with the local density approximation (LDA) and the generalized gradient approximation (GGA) separately. The plane-wave cutoff energy is set to 140 Ry for LDA and 55 Ry for GGA respectively through energy



test. Numerical integrations of Brillouin zone are performed by choosing a k-mesh of dimensions $10 \times 10 \times 10$. As for the calculation of the phonon spectral, we have selected a small q mesh of dimensions $4 \times 4 \times 4$ in force constant calculation.

The WZ structure of BN is modeled as Figure 1. The optimized values of the lattice constant are listed in Table I, which are close to the previous theoretical [11, 12] and experimental data [13].

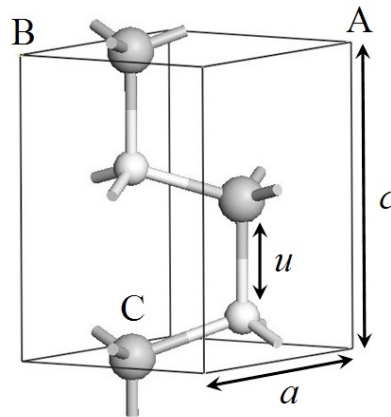


Figure 1. Wurtzite structures of BN. White balls represent B atoms and the dark gray balls N atoms. The lattice parameter a and c show as above.

Table I. The basic physical parameters of WZ-BN in the calculation compare with other theories and the experimental data

	$a(\text{\AA})$	$c(\text{\AA})$	c/a
This work ^{LDA}	2.51	4.12	1.639
This work ^{GGA}	2.55	4.23	1.661
Theory ^[11]	2.54	4.17	1.642
Theory ^[12]	2.53	4.19	1.654
Experiment ^[13]	2.56	4.23	1.656

3. Result and discussion

3.1. Band structures and density of states

Figures 2 and 3 show BN band structures and density of states (DOS) obtained by LDA and GGA, respectively. It is found that the calculated bands by GGA are slightly lower than those by LDA. The results also indicate that the BN is the indirect band gap semiconductor. The top valence band splits up into 3 sub-bands.

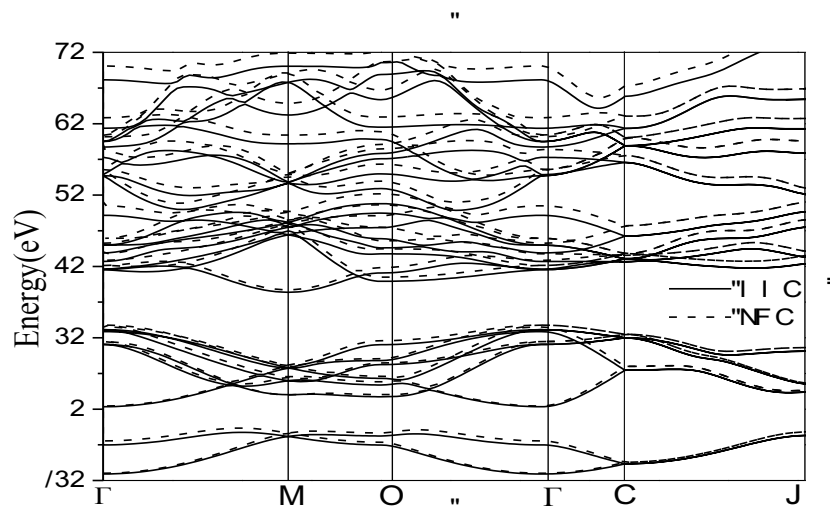


Figure 2. Band structure of WZ-BN obtained by GGA (solid line) and LDA (dash line).

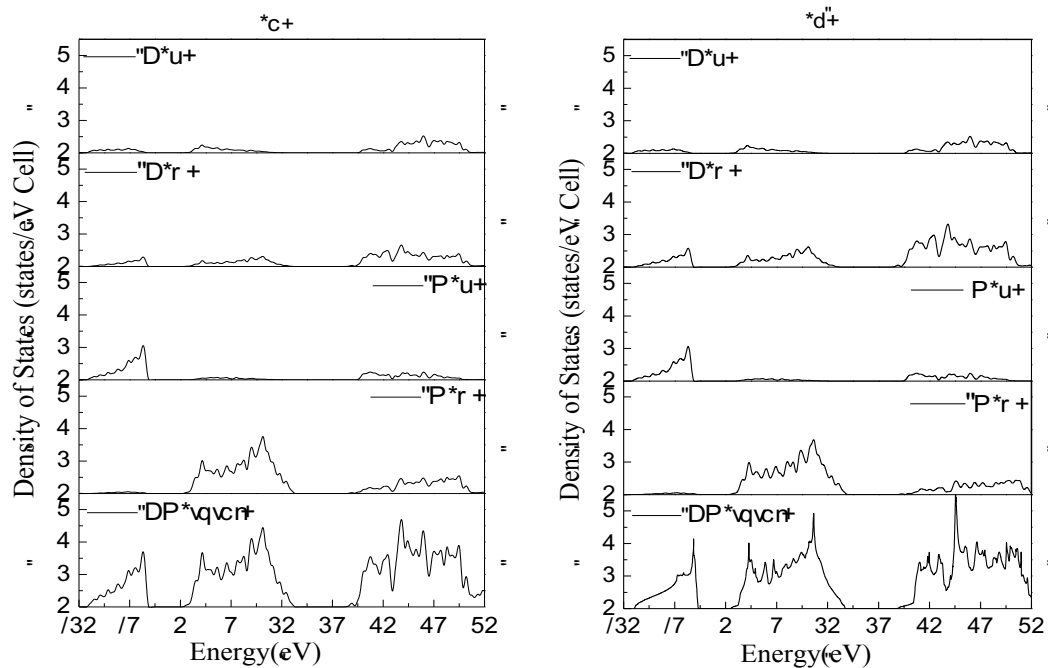


Figure 3. Total and part DOSs of WZ-BN by (a) GGA and (b) LDA calculations. B(s) stands for B atom 2s state, B (p) for B atom 2p state as well as N atoms.

One can also see that the valence band are mostly dominated by B-2s, 2p, N-2p electronic states and little N-2s electronic states, but the conduction band comes from B-2s, 2p and a little N-2s, 2p electron. The conclusions are consistent with other theoretical results.

3.2. Phonon dispersion curves

The calculated phonon dispersion curves and DOS of WZ-BN are plotted in figure 4. Due to the crystal primitive cell of WZ structure includes 4 atoms, consequently there is a splitting of the transverse optical (TO) and longitudinal optical (LO) phonon branches. It is expected that there are 12 branches of phonon modes, i.e. 3 branches of acoustic phonon modes and 9 branches of optical phonon modes. However, the phonon branches will degenerate in the different high symmetry points in the BN of hexagonal structure. For example, the phonon modes in the point A degenerate into only 4 modes, and there are 8 phonon modes at Γ point.

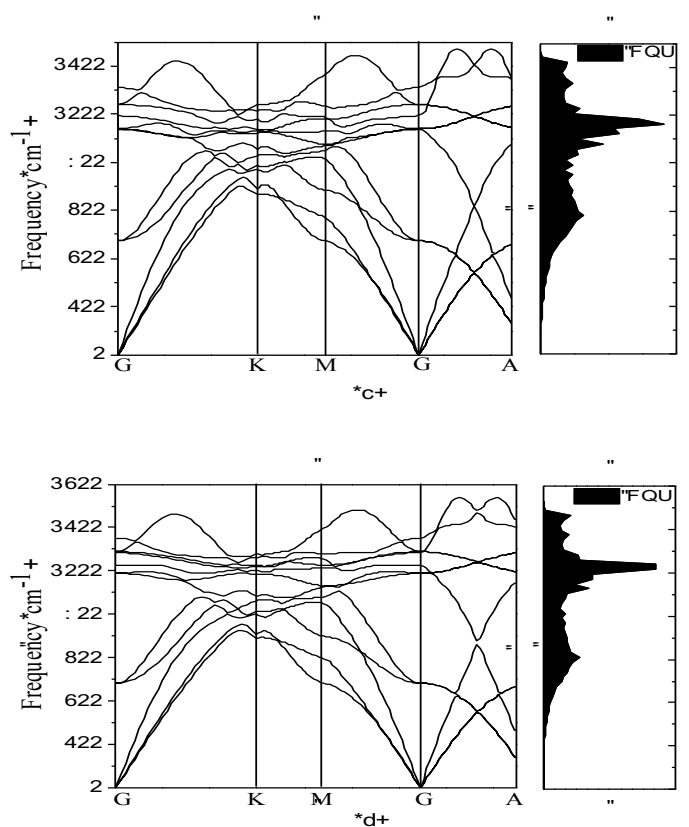


Figure 4. Phonon dispersion curves and DOSs of WZ-BN by (a) GGA and (b) LDA calculations.

As is known, a phonon band-gap can be found from the dispersion curves and DOS if the mass difference between the positive and negative ions in a primitive cell is obvious. However, there are no any gaps between the optical and acoustic branches of phonon modes in figure 4, since the masses of the different ions in BN are close to each others.

The calculated phonon frequencies at the Γ point in this work are listed in Table II. The corresponding results given by previous theories are also listed partly for comparison. As we know, the A_1 and E_1 mode have the Raman and infrared activities, E_2 modes only possess the infrared activity, and B_1 is matt lamination [12]. It is seen that the calculated values of the corresponding phonon frequencies by LDA are slight higher than those by GGA. Our computational results are close to the previous theories.

Table II. The calculated phonon frequencies at the Γ point for BN in wurtzite structure by LDA and GGA as well as some other theories and experimental data. The frequencies are measured in cm^{-1}

	E_2^l	B_1^l	$A_1(\text{TO})$	$E_1(\text{TO})$	E_2^h	B_1^h	$A_1(\text{LO})$	$E_1(\text{LO})$
This work ^{LDA}	482	989	992	1024	1084	1088	1090	1151
This work ^{GGA}	474	936	939	941	994	1040	1044	1112
Theory ^[14]	447	918	988	1024	948	1179	1258	1286
Theory ^[15]			1006	1053			1258	1286
Experiment ^[9]	310						1364	1364

3.3. Dielectric properties based on phonons

The Born effective charge tensor is diagonalizable and simplified into two values $\vec{Z}_{xx}^* = \vec{Z}_{yy}^* = \vec{Z}_p^*$ and \vec{Z}_\perp^* (Parallel and perpendicular to c-axis of the hexagonal structure respectively) because of the higher symmetry of the wurtzite structure. The similar form is received for the static dielectric tensor. The calculated results are listed in Table II.

Table III. The born effective charge and the static dielectric tensors

Z_p^*	Z_\perp^*	ϵ_p^*	ϵ_\perp^*
1.97	1.87	4.71	4.52
2.81	2.68	6.07	5.88

It is clearly seen that the parallel components of the Born effective charge and static dielectric tensors are greater than the perpendicular ones. The results embody the anisotropy of the spontaneous polarization of WZ-BN.

3.4. Thermodynamic properties based on phonon spectra

Thermodynamic properties of the lattice system can be obtained by calculating the thermodynamic functions using the phonon dispersion results [16]. We have performed the computations for some main thermodynamic functions, such as the inner energy, free energy, specific heat and entropy for the WZ-BN lattice system. One code of PWscf with the quasi harmonic approximation (QHA) is used in the calculation. The obtained results for the entropy S and the constant-volume specific heat C_V as functions of the temperature based on GGA and LDA are respectively plotted in figure 5. It is seen that the specific heat presents the T^3 -rule at low temperature and tend to a certain value when the temperature is high enough. The calculated results coincide with experimental and theoretical conclusions. Both the values of S and C_V by LDA are slightly lower than those by GGA, because the

former gets the smaller phonon density of states.

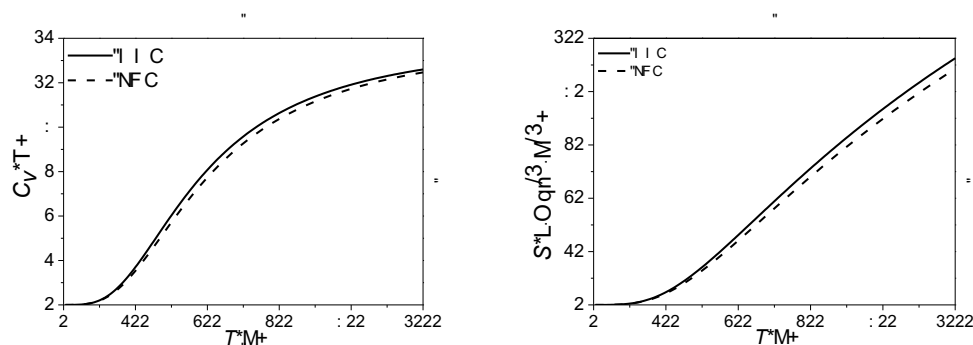


Figure 5. Entropy and constant-volume specific heat by GGA (solid line) and LDA (dash line), respectively. The specific heat is measured in $R = 8.31 \text{ J Mol}^{-1} \text{ K}^{-1}$.

4. Conclusion

In this work, we have applied first-principle calculation with two different pseudo potentials, LDA and GGA, to study the electronic states and the lattice dynamics of BN in wurtzite structures. The energy band structure of electrons and the phonon dispersion characteristics as well as the dielectric and thermal properties are discussed. The calculated results are in agreement with the zone-center Raman measurements and the previous ab initio calculations.

5. Acknowledgments

This work was supported in part by the PhD Progress Foundation of Higher Education Institutions of China (20111501110003), Natural Science Foundation of Inner Mongolia (No. 2011MS0105) and Talent Development Foundation of Inner Mongolia.

References

- [1] Carling K, Wahnström G, Mattsson T R, et al. 2000 *Physical review letters*. **85**, 3862
- [2] Kim K, Lambrecht W R L, Segall B 1996 *Physical Review B*. **53**, 16310
- [3] Haubner R, Wilhelm M, Weissenbacher R, et al. 2002 *Springer Berlin Heidelberg*
- [4] Lorenz H, Orgzall I 2004 *Acta materialia*. **52**, 1909-1916
- [5] Mosuang T E, Lowther J E 2002 *Journal of Physics and Chemistry of Solids*. **63**, 363-368
- [6] Michel K H, Verberck B 2011 *Physical Review B*. **83**, 115328
- [7] Tohei, T., Kuwabara, A., Oba, F., & Tanaka, I. 2006 *Physical Review B*. **73**, 064304
- [8] Ohba, N., Miwa, K., Nagasako, N., & Fukumoto, A. 2001 *Physical Review B*, **63**, 115207
- [9] Reich, S., Ferrari, A. C., Arenal, R. et al. 2005 *Physical Review B*. **71**, 205201
- [10] Giannozzi P, Baroni S, Bonini P, etc. 2009 *J. Phys Condens. Matter*. **21**, 395502-395521
- [11] Lawniczak-Jablonska K, Suski T, Gorczyca I, et al. 2000 *Physical Review B*. **61**, 16623
- [12] Shimada, K., Sota, T., & Suzuki, K. 1998 *Journal of applied physics*, **84**, 4951-4958.
- [13] Sōma, T., Sawaoka, A., & Saito, S. 1974 *Materials Research Bulletin*. **9**, 755-762
- [14] Tütüncü H M, Srivastava G P 2000 *Physical Review B*. **62**, 5028
- [15] Kim K, Lambrecht WRL and Segall B. 1996 *Phys. Rev. B*. **53**, 16310-16326
- [16] Van De Walle, A., & Ceder, G. 2002 *Reviews of Modern Physics*. **74**, 11